Supramolecular Chemistry
Publication details, including instructions for authors and subscription information:
http://www.informaworld.com/smpp/title~content=t713649759

Mini-zippers: Determination of oligomer effects for the assembly of photoactive supramolecular rod/stack architectures on gold nanoparticles and gold electrodes

Marco Lista[a]; Naomi Sakai[a]; Stefan Matile[a]
[a] Department of Organic Chemistry, University of Geneva, Geneva, Switzerland

To cite this Article Lista, Marco , Sakai, Naomi and Matile, Stefan(2009) 'Mini-zippers: Determination of oligomer effects for the assembly of photoactive supramolecular rod/stack architectures on gold nanoparticles and gold electrodes', Supramolecular Chemistry, 21: 3, 238 — 244
To link to this Article: DOI: 10.1080/10610270802516617
URL: http://dx.doi.org/10.1080/10610270802516617

Supramolecular Chemistry
Vol. 21, Nos. 3–4, April–June 2009, 238–244

Taylor & Francis
Taylor & Francis Group

Mini-zippers: Determination of oligomer effects for the assembly of photoactive supramolecular rod/stack architectures on gold nanoparticles and gold electrodes

Marco Lista, Naomi Sakai and Stefan Matile*

Department of Organic Chemistry, University of Geneva, Geneva, Switzerland

(*Received 9 July 2008; final version received 28 September 2008*)

The objective of this study was to evaluate the importance of oligomer effects for the assembly of functional rod/stack architectures on solid substrates. The original approach to the 'zipper assembly' of functional rod/stack architectures focused on *p*-quaterphenyl initiators and *p*-octiphenyl propagators with naphthalenediimides (NDIs) attached along their scaffold. Here, we describe the synthesis and evaluation of 'mini-zippers' composed of the homologous biphenyl initiators and *p*-quaterphenyl propagators. Whereas the synthesis of shorter oligomers is less demanding, their less efficient assembly on gold nanoparticles and electrodes produces overall less convincing results. On gold nanoparticles, the increase in absorption during the assembly of mini-zippers stops around notional π-stacks of six NDIs; original zippers provide access to at least three times higher NDI absorption and notional π-stacks of 30 NDIs before reaching saturation. On gold electrodes, the increase in photocurrent per NDI with mini-zippers is 50% of that with original zippers. Moreover, photocurrents of mini-zippers saturate at notional π-stacks of 40 NDIs, whereas original zippers can produce larger photocurrents and notional π-stacks of 80 NDIs without reaching saturation. These results suggest that for functional supramolecular rod/stack architectures, oligomer effects are essential and cannot be ignored.

Keywords: self-assembly; layer-by-layer assembly; photocurrent; artificial photosynthesis; length dependence; oligomer effects

Introduction

The emergence of new characteristics when structural motifs are repeated several times is a fundamental phenomenon in chemistry and biology. Oligomer effects contribute significantly not only to physical properties such as colour or conductivity but also to the biological functional systems that are obtained from DNA, proteins, polysaccharides or lipids and their synthetic mimics. In folding, self-assembly and molecular recognition, oligomer effects often originate from multivalency, where small energy gains from weak intra- or inter-molecular interactions are repeated in an overadditive (i.e. cooperative) manner to achieve significant impact (*1–17*). Oligomer effects assure the existence of not only structures as common as α-helices, β-sheets or DNA duplexes but also their many synthetic analogues and mimics (*8–17*). Their functional relevance is ubiquitous and still continues to surprise in more complex systems such as lipid bilayer membranes (*15*, *17*).

Rigid-rod molecules are a unique family of unfoldable oligomers with backbone conformations that do not depend on oligomer effects (*18*). Their introduction as privileged scaffolds of supramolecular multifunctional architectures was of interest to exploit oligomer effects for self-assembly and molecular recognition, translocation and transformation without complications from length-dependent conformational changes of the rigid-rod scaffold itself (*19*). With rigid-rod architectures, oligomer effects have been reported for the self-assembly into artificial β-barrels (*1*), the interaction with lipid bilayer membranes (*2–4*) and the formation of proton channels (*3–5*). In this report, we describe significant oligomer effects for the zipper assembly of photoactive rigid-rod architectures on solid substrates.

The zipper assembly has been introduced to contribute a new approach towards supramolecular functional cascade architectures with interdigitating intra- and inter-layer recognition motifs on solid substrates (Figure 1; *6*, *7*). For the envisioned rod/stack architectures such as Au-***b***-**B**-***B***, *p*-oligophenyls (POPs; *1–7, 18*) were selected as rods and naphthalenediimides (NDIs; *20–41*) as stacks. NDIs (*20*) were attractive because their frontier orbital energy levels can be varied without global structural changes (*6, 7, 21–29*), and their planarity and π-acidity (*30, 31*) support the formation of *n*-semiconducting (*29, 32–34*) π-stacks (*35–41*) next to the *p*-semiconducting POP rods (*6, 7, 25–27, 39*). Access to such supramolecular cascade *n*/*p*-heterojunctions would be of general interest to maximise the efficiency of optoelectronic devices (*7, 42, 43*). The blue, red fluorescent bNDIs with alkylamine core substituents

*Corresponding author. Email: stefan.matile@unige.ch; www.unige.ch/sciences/chiorg/matile/

ISSN 1061-0278 print/ISSN 1029-0478 online

DOI: 10.1080/10610270802516617
http://www.informaworld.com

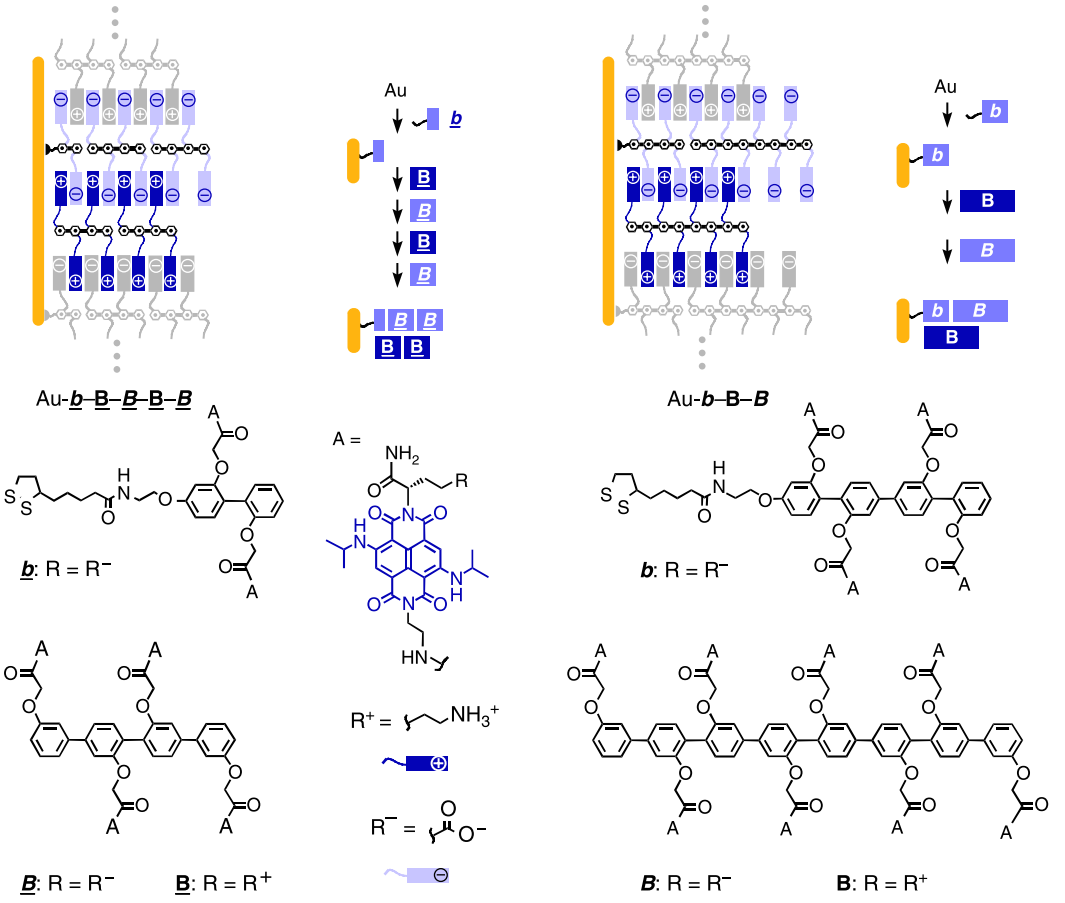

Figure 1. The assembly of functional 'mini-zippers' such as Au-**b**–**B**–***B***–**B**–***B*** from minimalist biphenyl initiators **b** and *p*-quaterphenyl propagators **B** and ***B*** on gold (*left*) compared to the zipper assembly of the original functional 'full-length' rod/stack architectures such as Au-***b***-**B**-***B*** from *p*-quaterphenyl initiators ***b*** and *p*-octiphenyl propagators **B** and ***B*** (*right*). Neighbouring 'zippers' are coloured in grey for clarity. All suprastructures are speculative representations and shown with the only intention to illustrate the concepts (cf. Figure 2).

used in this study are oxidisable and reducible, and they exhibit ultrafast quantitative photoinduced charge separation that lasts for 61 ps in monomeric **B** (*25*) and more than 1 ns in π-stack architectures (*27*).

For the zipper assembly (*6, 7*), NDIs from neighbouring POPs are designed to interdigitate and form face-to-face π-stacks along the rigid-rod scaffolds. Intrastack hydrogen-bonded chains and interstack ion pairing should further orient and stabilise the NDI stacks (*6, 39*). The intralayer interdigitation of the NDIs should then be complemented by interlayer interdigitation of the POP scaffolds (*1, 6, 7*). To initiate this process, initiator ***b*** with a disulphide at one terminus is linked to a gold surface (Figure 1; *6*). Binding of propagator **B** to the obtained Au-***b*** then occurs by π-stacking of the four anionic NDIs of *p*-quaterphenyl ***b*** with four cationic NDIs from *p*-octiphenyl **B**. The other four NDIs of double-length *p*-octiphenyl **B** remain as 'sticky ends' at the surface of the obtained Au-***b***-**B** to zip up with four cationic NDIs of the anionic propagator ***B***. The resulting anionic sticky ends of zipper Au-***b***-**B**-***B*** can zip up with four NDIs of cationic propagator **B** to give Au-***b***-**B**-***B***-**B**, and so on. Confirmation of the envisioned zipper architectures on the structural level is very difficult, and the existence of alternative or mixed assemblies cannot be excluded at this stage (Figure 2). However, functional significance is readily confirmed by increasing photocurrents with each new zipper assembly, and the existence of sticky ends was supported by the inhibition of zipper growth with *p*-quaterphenyl terminators ***b*** (*6*).

This report focuses on the assembly of mini-zippers such as Au-**b**–**B**–***B***–**B**–***B*** from homologous biphenyl initiators and *p*-quaterphenyl propagators (Figure 1). The objective was to assess the importance of oligomer effects, which is the constructive combination of cooperativity and multivalency (*1–17*), for the assembly of photoactive rod/stack architectures such as Au-***b***-**B**-***B*** from original *p*-quarterphenyl initiators ***b*** and *p*-octiphenyl propagators **B** and ***B*** (*6, 7*). The length dependence found provides experimental support for the critical importance of oligomer effects for the creation of supramolecular functional architectures (*6, 7*) such as photosystem Au-***b***-**B**-***B***.

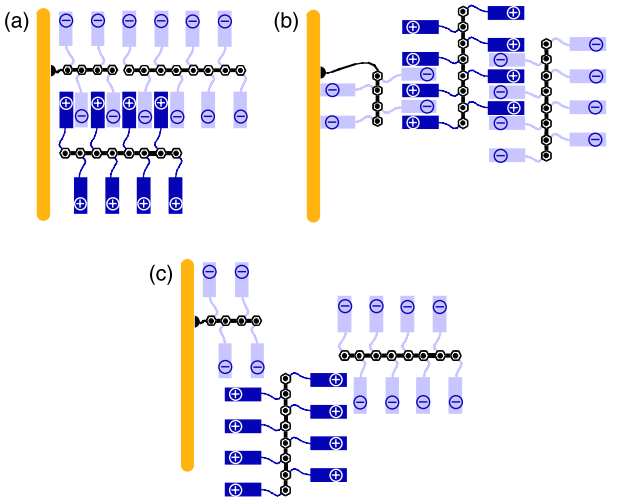

Figure 2. Conceivable suprastructural motifs for Au-***b***-**B**-***B*** include not only (a) 'zippers' with inter- and intralayer interdigitation by rods and stacks, but also (b) 'horizontal' alternatives without interdigitating rods and (c) less-ordered layers without interdigitating rods and stacks.

Results and discussion

The three components ***b***, **B** and ***B*** needed to study the assembly of mini-zippers were synthesised following, essentially, the procedure developed for the original homologues ***b***, **B** and ***B***. The early steps of the synthesis of the biphenyl initiator ***b*** from resorcinol **1** have been reported (Scheme 1(a)) (*6*).

In brief, Williamson monoetherification with bromide **2** followed by regiospecific iodination, etherification with bromide **3** and Pd-catalysed aromatic substitution with pinacolborane gave boronate **4**. Suzuki coupling with the aryliodide **5** provided biphenyl **6**. After hydrogenolytic deprotection, the obtained amine **7** was coupled with HATU-activated lipoic acid **8**. Acid-catalysed deprotection of biphenyl diester **9** gave diacid **10**. The blue NDI **11** was prepared applying the newly introduced, convenient, mild and rapid route via direct bromination of dianhydride **12** with dibromoisocyanuric acid (*28*). Diamide formation with HATU-activated diacid **10** and amine **11** followed by acid-catalysed hydrolysis of the *tert*-butyl esters in **13** gave initiator ***b***.

The early steps of the synthesis of the minimalist *p*-quaterphenyl propagators ***B*** and **B** from biphenyl **14** followed the routine *p*-octiphenyl synthesis (Scheme 2; *44*). In brief, nucleophilic aromatic substitution with KI was followed by BuLi-mediated replacement of one of the two iodides with a proton. The oxidative Ullman coupling of the resulting iodobiphenyls mediated by BuLi and $CuCl_2$ and side-chain modification along the obtained *p*-quateranisol with BBr_3, bromoacetate **3** and TFA gave the *p*-quaterphenyl **15** with carboxylic acids placed along the scaffold (*45*). Reaction with NDI amine **11** followed by deprotection

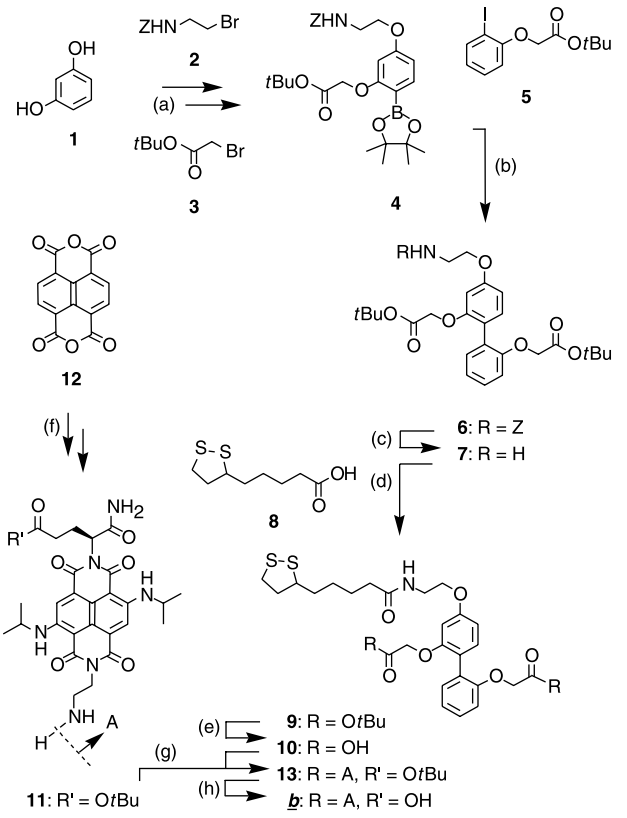

Scheme 1. (a) 1. **2**, Cs_2CO_3, DMF, 18 h, 40°C, 51%; 2. I_2, AgOTf, $CHCl_3$, 1.5 h, rt, 47% (quant. conversion yield); 3. **3**, Cs_2CO_3, DMF, 1 h, 60°C, 97%; 4. $PdCl_2$(dppf), pinacolborane, TEA, CH_3CN, 1 h, 90°C, 87% (*6, 7*); (b) **5**, $PdCl_2$(dppf), Na_2CO_3, toluene–EtOH, 1 h, 90°C, 70%; (c) H_2, Pd–C (10%), EtOAc/MeOH, 4 h, rt; (d) **8**, HATU, TEA, DMF, 15 min, rt, 65% (from **6**); (e) TFA, CH_2Cl_2, rt, quant.; (f) 1. dibromoisocyanuric acid, oleum, 6 h, rt (product mixture); 2. alloc-ethylenediamine, H-Glu(*t*-Bu)-NH_2, AcOH, 12 h, 80°C, two steps 12%; 3. *i*-$PrNH_2$, 24 h, rt, 60%; 4. $PdCl_2(PPh_3)_2$, Bu_3SnH, *p*-NO_2-phenol, quant. (*28*); (g) HATU, di-*t*-Bu-pyridine, TEA, DMF, 2 h, rt, 31% and (h) TFA, CH_2Cl_2, quant.

of *p*-quaterphenyl **16** gave the anionic propagator ***B***, reaction with NDI amine **17** followed by deprotection of **18** gave the cationic propagator **B**.

The assembly of mini-zippers was studied first on gold nanoparticles. Freshly prepared citrate-stabilised gold nanoparticles ($d \approx 13$ nm, Figure 3(a)) were coated with biphenyl initiator ***b***, following the procedure developed previously for the original *p*-quaterphenyl initiator ***b*** (Figure 3(b)).

The obtained anionic mini-Au-***b*** was incubated with the cationic propagators **B** in phosphate buffer, and the obtained mini-Au-***b***–**B** was separated from unbound **B** by repeated centrifugation (Figure 3(c)). The transformation of mini-Au-***b*** to mini-Au-***b***–**B** was supported by an increasing NDI absorption around 630 nm in absorption spectra. The coinciding bathochromic shift of the surface plasmon resonance (SPR) band near 520 nm provided accurate information for the increase in layer thickness during the

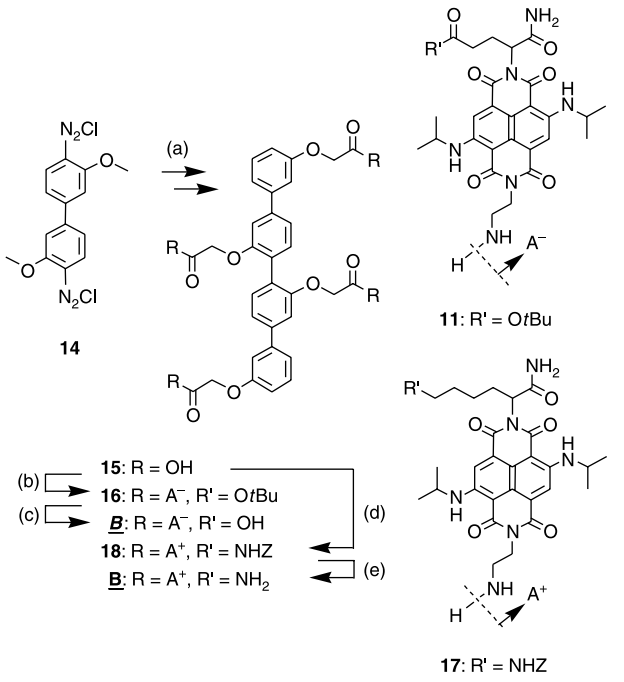

Scheme 2. (a) 1. KI, 70%; 2. *n*-BuLi, 67%; 3. *n*-BuLi, $CuCl_2$, 64%; 4. BBr_3; 5. **3**, Cs_2CO_3, DMF, 1 h, 60°C; 6. TFA, CH_2Cl_2, quant. (*45*); (b) **11**, HATU, di-*t*-Bu-pyridine, TEA, DMF, 14 h, rt, 40%; (c) TFA, CH_2Cl_2, quant.; (d) **17**, HATU, di-*t*-Bu-pyridine, TEA, DMF, 14 h, rt, 35% and (e) TFA, CH_2Cl_2, quant.

transformation of mini-Au-***b*** to mini-Au-***b***–**B** (*46, 47*). This procedure was repeated several times with anionic propagator ***B*** and cationic propagator **B**, and the changes in the absorption spectra were recorded with regard to both the NDI absorption (Figure 4, ■) and the bathochromic effect of the SPR band (Figure 4, •). However, the changes in absorption became increasingly less significant.

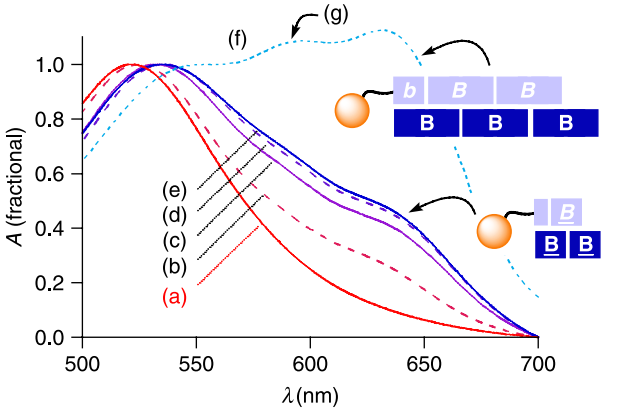

Figure 3. Changes in absorption during the formal assembly of mini-zipper Au-***b***–**B**–***B***–**B** (e) on gold nanoparticles compared to the previously reported (*6*) Au-***b*****-B-*B*-B-*B*-B** (f) with a new maximum around 600 nm (g). Intermediates: (a) Au; (b) Au-***b***; (c) Au-***b***–**B** and (d) Au-***b***–**B**–***B*** (all in 50% aqueous TFE, 100 mM NaCl and 10 mM phosphate).

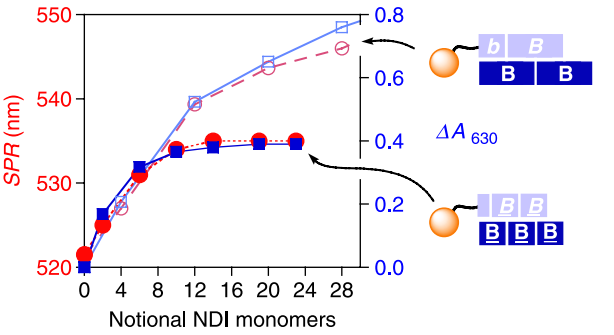

Figure 4. Zipper assembly on gold nanoparticles. Increase in NDI absorption ΔA at 630 nm (Y_2, blue, squares) and bathochromism of the SPR band from 520 nm (Y_1, red, circles) during the formal assembly of mini-zipper Au-***b***–**B**–***B***–**B**–***B***–**B** (filled symbols) compared to the previously reported (*6*) Au-***b*****-B-*B*-B** (empty symbols), all in 50% aqueous TFE, 100 mM NaCl and 10 mM phosphate. For the sake of comparison, the changes are given as a function of the number of theoretical layers of NDI monomers (2 per ***b***, 4 per **B**, ***B*** and ***b*** and 8 per **B** and ***B***). This is necessarily an overestimate, with its extent reporting on the yield of the zipper assembly. Each data point represents a new layer of assembly.

Saturation occurred around Au-***b***–**B**–***B*** (Figure 3(d)) and Au-***b***–**B**–***B***–**B** (Figures 3(e) and 4, ■ and •). At saturation with mini-zippers, the NDI absorption was still clearly less intense than the SPR band (Figure 3(e)). With original zippers, this saturation behaviour was reached neither for NDI absorption (Figure 4, □) nor for SPR bathochromism (Figure 4, ○) (*6*). The maximal absorption reached with mini-zipper Au-***b***–**B**–***B***–**B** was at least three times weaker than that accessible with original zipper Au-***b*****-B-*B*-B-*B*-B** (Figure 3(f)). The maximal absorption obtained with mini-zippers was insufficient to detect the appearance of a hypsochromic maximum around 600 nm. Contrary to the situation with original zippers (Figure 3(g)), this qualitative support for face-to-face π-stacking (*6*, *25*, *48*) of the NDIs in the obtained rod/stack architecture could not be secured for mini-zippers. Although impossible to determine at this stage, we assume that this occurs because of insufficient absorption rather than lacking order. Attempts to improve the assembly of mini-zippers on gold nanoparticles by changing ionic strength and pH of the buffer failed.

Before saturation of the mini-zipper around eight notional layers of NDI monomers, zipper growth was independent of oligomer length (Figure 4). This result underscored the central importance of oligomer effects to assure supramolecular organisation over long distances, whereas the organisation of thinner films is clearly less demanding to control (*vide infra*).

The zipper assembly on gold electrodes was evaluated next. Dipping of the electrode into a solution of biphenyl initiator ***b*** in water (1 mM sodium phosphate, pH 7) and TFE (1:1) at room temperature caused complete inhibition of electrochemical ferricyanide reduction within one week

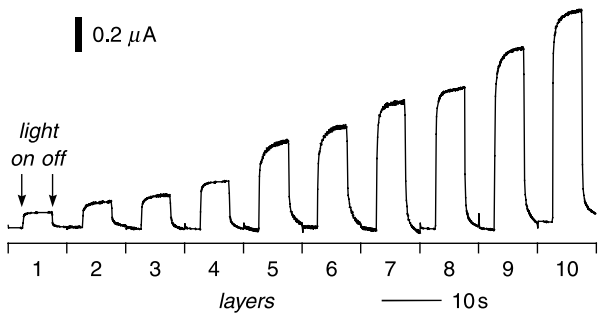

Figure 5. Change in photocurrent during the assembly of mini-zipper Au-***b***–**B**–***B***–**B**–***B***–**B**–***B***–**B**–***B***–**B** on gold electrodes (conditions: **2**, **3** (~10 μM) in TFE/H_2O (0.5 mM $Na_nH_{3-n}PO_4$, 1 M NaCl, pH 7) 1:1, rt, 14 h; rinsed with H_2O and EtOH).

of incubation. This result demonstrated that the coverage of the surface with anionic initiator ***b*** is sufficient to hinder the ferricyanide to reach to the gold electrode.

Irradiation of the obtained Au-***b*** electron acceptors in the presence of triethanolamine as the sacrificial electron donor and a Pt electrode as the cathode caused the appearance of a small photocurrent (Figure 5, layer 1). The assembly of mini-zippers by repeated dipping of Au-***b*** into first cationic and then anionic propagators **B** and ***B***, respectively, gave the expected increase in photocurrent (Figures 5 and 6, ○).

Highest photocurrent was observed for Au-***b***–**B**–***B***–**B**–***B***–**B**–***B***–**B**–***B***–**B**, a mini-zipper theoretically composed of 10 interdigitating *p*-POP layers. Beginning with

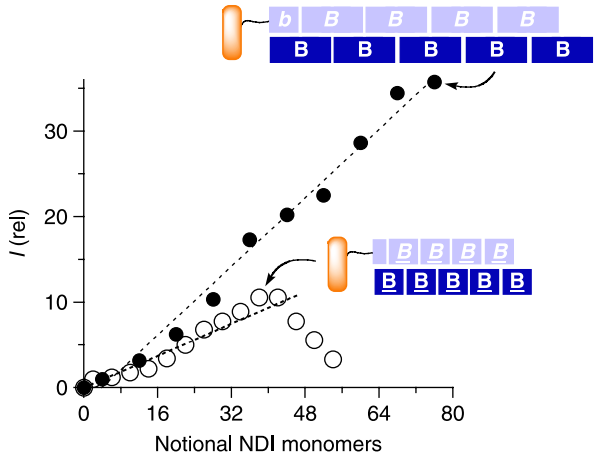

Figure 6. Zipper assembly on gold electrodes. Dependence of the relative photocurrent on the number of theoretical layers of NDI monomers for mini-zipper Au-***b***–**B**–***B***–**B**–***B***–**B**–***B***–**B**–***B***–**B** (○) compared to the original (*6*) zipper Au-***b***-**B**-***B***-**B**-***B***-**B**-***B***-**B** (•). The theoretical number of NDI monomers (2 per added layer of ***b***, 4 per **B**, ***B*** and ***b***, and 8 per **B** and ***B***) is an overestimate, with not only the yield of the zipper assembly but also other parameters including supramolecular architecture accounting for the difference. Each data point represents a single step of assembly. The linear curve fit is added only to guide the eye, the last two data points of the mini-zipper are not included.

layer 11, photocurrents started to decrease (Figure 6, ○). This 'post-saturation' behaviour of mini-zippers (i.e. decreasing photocurrent with increasing number of layers after a critical film thickness) could originate from cooperative increase in disorder with increasing zipper size at overcritical film thickness. Such long-range disorder might induce the disassembly of zipper components. Attractive alternative explanations of zipper inactivation at overcritical film thickness reach from reduced lifetime of photoinduced charge separated states (*27*) to hindered electron transfer through disordered NDI stacks. The individual importance of these possible explanations of the decreasing photocurrents at overcritical film thickness was not further investigated. Similar 'post-saturation' decrease in photoactivity with increasing number of layers has been reported previously for the less-ordered architectures obtained by the traditional layer-by-layer assembly of polyelectrolytes (*49*). Consistent with the results from gold nanoparticles, the saturation and 'post-saturation' behaviour of photocurrents obtained by the zipper assembly underscored the particular importance of oligomer effects to assure the long-range supramolecular organisation of films at overcritical thickness.

At the same number of around 40 NDIs theoretically stacked on top of each other, the photocurrents obtained with original zippers showed no sign of saturation or decrease (Figure 6, •). Saturation was also not approached with continuing assembly of original zippers up to double size with theoretically 80 NDIs stacked on top of each other. Compared to mini-zippers, original zippers provided access to nearly four times higher photocurrents (Figure 6, • vs. ○). Qualitative linear curve fit excluding saturation revealed that the increase in photocurrent per NDI with original zippers is more than twice that of mini-zippers (Figure 6, dotted lines). Early saturation and decrease in photocurrents, much smaller maximal photocurrent as well as more than two times smaller increase in photocurrent per NDI all suggested that the assembly of mini-zippers is less efficient and/or produces less-organised rod/stack architectures compared to original zippers (Figures 5 and 6). This interpretation was further supported by the inaccessibility of 'thick' films on gold nanoparticles with mini-zippers (Figures 3 and 4).

Conclusion

We conclude that the synthesis and study of mini-zippers appears ideal to explore the significance of oligomer effects for the zipper assembly. Rod/stack architectures constructed from rigid-rod scaffolds half as long as in the original systems are demonstrated to exhibit clearly reduced activity. Maximal accessible photocurrents are clearly smaller, and the increase in photocurrent per NDI is more than two times smaller. With mini-zippers, photocurrents saturate and start to decrease with around 40 π-stacked NDIs, whereas original zippers do not show

saturation at 80 π-stacked NDIs. On gold nanoparticles, increasing NDI absorption and SPR bathochromism is observed for original zippers beyond 30 π-stacked NDIs (Au-***b***-**B**-***B***). For mini-zippers, absorption and SPR changes stop around 6 π-stacked NDIs (Au-***b***−**B**).

Taken together, these remarkably consistent results demonstrate the importance of oligomer effects in the zipper assembly. Higher photocurrent increase per chromophore with longer scaffolds suggests that oligomer effects contribute to the efficiency of the zipper assembly. Higher maximal absorption and maximal photocurrent with longer scaffolds suggest that oligomer effects also account for the stability of the resulting zipper architectures. The saturation behaviour seen with shorter scaffolds, eventually followed by a stunning decrease in photocurrent with increasing assembly, suggests that the organisation of mini-zippers is simply not very good.

This compelling experimental evidence in support of significant oligomer effects is in excellent agreement with the existence of interdigitating intralayer (horizontal) and interlayer (vertical) recognition motifs envisioned with the zipper assembly (Figure 2(a)). However, it is important to reiterate that the existence of oligomer effects does not prove the existence of zipper architectures as designed (Figures 1 and 2(a)). For instance, rod/stack architectures without interdigitating rods (Figure 2(b)) are likely to exhibit oligomer effects as strong as the envisioned zipper architectures (Figure 2(a)). Whereas structural aspects thus remain to be explored, this study fully clarifies the functional importance of oligomer effects in the zipper assembly of functional rod/stack architectures in solid substrates. The conclusion that the synthesis of higher oligomers is unavoidable to access significant function is consistent with previous results from supramolecular functional systems.

Experimental section

The synthesis and evaluation of truncated homologues was accomplished by following and thus validating the procedures developed with the original zipper architectures described in Ref. (*6*). Complete experimental details can be found in the Supporting Information, available online.

Acknowledgements

We thank D.-H. Tran for contributions to synthesis, and the University of Geneva and the Swiss NSF for financial support.

References

(1) Das, G.; Matile, S. *Chirality* **2001**, *13*, 170–176.
(2) Ghebremariam, B.; Sidorov, V.; Matile, S. *Tetrahedron Lett.* **1999**, *40*, 1445–1448.
(3) Ni, C.; Matile, S. *Chem. Commun.* **1998**, *33*, 755–756.
(4) Weiss, L.A.; Sakai, N.; Ghebremariam, B.; Ni, C.; Matile, S. *J. Am. Chem. Soc.* **1997**, *119*, 12142–12149.
(5) Sakai, N.; Brennan, K.C.; Weiss, L.A.; Matile, S. *J. Am. Chem. Soc.* **1997**, *119*, 8726–8727.
(6) Sakai, N.; Sisson, A.L.; Bürgi, T.; Matile, S. *J. Am. Chem. Soc.* **2007**, *129*, 15758–15759.
(7) Sisson, A.L.; Sakai, N.; Banerji, N.; Fürstenberg, A.; Vauthey, E.; Matile, S. *Angew. Chem. Int. Ed.* **2008**, *47*, 3727–3729.
(8) Hill, D.J.; Mio, M.J.; Prince, R.B.; Hughes, T.S.; Moore, J.S. *Chem. Rev.* **2001**, *101*, 3893–4012.
(9) Gellman, S.H. *Acc. Chem. Res.* **1998**, *31*, 173–180.
(10) Mammen, M.; Choi, S.K.; Whitesides, G.M. *Angew. Chem. Int. Ed.* **1998**, *37*, 2755–2794.
(11) Baldini, L.; Casnati, A.; Sansone, F.; Ungaro, R. *Chem. Soc. Rev.* **2007**, *36*, 254–266.
(12) Crespo-Biel, O.; Ravoo, B.J.; Reinhoudt, D.N.; Huskens, J. *J. Mater. Chem.* **2006**, *16*, 3997–4021.
(13) Badjic, J.D.; Nelson, A.; Cantrill, S.J.; Turnbull, W.B.; Stoddart, J.F. *Acc. Chem. Res.* **2005**, *38*, 723–732.
(14) Kiessling, L.L.; Strong, L.E.; Gestwicki, J.E. *Ann. Rep. Med. Chem.* **2000**, *35*, 321–330.
(15) Ariga, K.; Kunitake, T. *Acc. Chem. Res.* **1998**, *31*, 371–378.
(16) Stone, M.T.; Heemstra, J.M.; Moore, J.S. *Acc. Chem. Res.* **2006**, *39*, 11–20.
(17) Sakai, N.; Matile, S. *J. Am. Chem. Soc.* **2003**, *125*, 14348–14356.
(18) Schwab, P.F.H.; Levin, M.D.; Michl, J. *Chem. Rev.* **1999**, *99*, 1863–1934.
(19) Sakai, N.; Mareda, J.; Matile, S. *Acc. Chem. Res.* **2005**, *38*, 79–87.
(20) Bhosale, S.V.; Jani, C.H.; Langford, S.J. *Chem. Soc. Rev.* **2008**, *37*, 331–342.
(21) Würthner, F.; Ahmed, S.; Thalacker, C.; Debaerdemaeker, T. *Chem. Eur. J.* **2002**, *8*, 4742–4750.
(22) Thalacker, C.; Röger, C.; Würthner, F. *J. Org. Chem.* **2006**, *71*, 8098–8105.
(23) Röger, C.; Würthner, F. *J. Org. Chem.* **2007**, *72*, 8070–8075.
(24) Blaszczyk, A.; Fischer, M.; von Hänisch, C.; Mayor, M. *Helv. Chim. Acta* **2006**, *89*, 1986–2005.
(25) Bhosale, S.; Sisson, A.L.; Talukdar, P.; Fürstenberg, A.; Banerji, N.; Vauthey, E.; Bollot, G.; Mareda, J.; Röger, C.; Würthner, F.; Sakai, N.; Matile, S. *Science* **2006**, *313*, 84–86.
(26) Bhosale, S.; Matile, S. *Chirality* **2006**, *18*, 849–856.
(27) Banerji, N.; Fürstenberg, A.; Bhosale, S.; Sisson, A.L.; Sakai, N.; Matile, S.; Vauthey, E. *J. Phys. Chem. B* **2008**, *112*, 8912–8922.
(28) Kishore, R.S.K.; Ravikumar, V.; Bernardinelli, G.; Sakai, N.; Matile, S. *J. Org. Chem.* **2008**, *73*, 738–740.
(29) Jones, B.A.; Facchetti, A.; Wasielewski, M.R.; Marks, T.J. *J. Am. Chem. Soc.* **2007**, *129*, 15259–15278.
(30) Gorteau, V.; Bollot, G.; Mareda, J.; Perez-Velasco, A.; Matile, S. *J. Am. Chem. Soc.* **2006**, *128*, 14788–14789.
(31) Gorteau, V.; Bollot, G.; Mareda, J.; Matile, S. *Org. Biomol. Chem.* **2007**, *5*, 3000–3012.
(32) Miller, L.L.; Mann, K.R. *Acc. Chem. Res.* **1996**, *29*, 417–423.
(33) Katz, H.E.; Lovinger, A.J.; Johnson, J.; Kloc, C.; Siegrist, T.; Li, W.; Lin, Y.Y.; Dodabalapur, A. *Nature* **2000**, *404*, 478–481.

(34) Morandeira, A.; Fortage, J.; Edvinsson, T.; Le Pleux, L.; Blart, E.; Boschloo, G.; Hagfeldt, A.; Hammarstrom, L.; Odobel, F. *J. Phys. Chem. C* **2008**, *112*, 1721–1728.
(35) Bhosale, S.; Sisson, A.L.; Sakai, N.; Matile, S. *Org. Biomol. Chem.* **2006**, *4*, 3031–3039.
(36) Lokey, R.S.; Iverson, B.L. *Nature* **1995**, *375*, 303–305.
(37) Iijima, T.; Vignon, S.A.; Tseng, H.R.; Jarrosson, T.; Sanders, J.K.M.; Marchioni, F.; Venturi, M.; Apostoli, E.; Balzani, V.; Stoddart, J.F. *Chem. Eur. J.* **2004**, *10*, 6375–6392.
(38) Mukhopadhyay, P.; Iwashita, Y.; Shirakawa, M.; Kawano, S.; Fujita, N.; Shinkai, S. *Angew. Chem. Int. Ed.* **2006**, *45*, 1592–1595.
(39) Talukdar, P.; Bollot, G.; Mareda, J.; Sakai, N.; Matile, S. *J. Am. Chem. Soc.* **2005**, *127*, 6528–6529.
(40) Hagihara, S.; Gremaud, L.; Bollot, G.; Mareda, J.; Matile, S. *J. Am. Chem. Soc.* **2008**, *130*, 4347–4351.
(41) Hagihara, S.; Tanaka, H.; Matile, S. *J. Am. Chem. Soc.* **2008**, *130*, 5656–5657.
(42) Würthner, F.; Chen, Z.; Hoeben, F.J.M.; Osswald, P.; You, C.-C.; Jonkheijm, P.; Herrikhuyzen, J.; Schenning, A.P.H.J.; van der Schoot, P.P.A.M.; Meijer, E.W.; Beckers, E.H.A.; Meskers, S.C.J.; Janssen, R.A.J. *J. Am. Chem. Soc.* **2004**, *126*, 10611–10618.
(43) Yamamoto, Y.; Fukushima, T.; Suna, Y.; Ishii, N.; Saeki, A.; Seki, S.; Tagawa, S.; Taniguchi, M.; Kawai, T.; Aida, T. *Science* **2006**, *314*, 1761–1764.
(44) Baumeister, B.; Sakai, N.; Matile, S. *Org. Lett.* **2001**, *3*, 4229–4232.
(45) Litvinchuk, S.; Matile, S. *Supramol. Chem.* **2005**, *17*, 135–139.
(46) Haes, A.J.; Zou, S.; Schatz, G.C.; Van Duyne, R.P. *J. Phys. Chem. B* **2004**, *108*, 109–116.
(47) Liu, G.L.; Yin, Y.; Kunchakarra, S.; Mukherjee, B.; Gerion, D.; Jett, S.D.; Bear, D.G.; Gray, J.W.; Alvisatos, A.P.; Lee, L.P.; Chen, F.F. *Nat. Nanotech.* **2006**, *1*, 47–52.
(48) Giaimo, J.M.; Gusev, A.V.; Wasielewski, M.R. *J. Am. Chem. Soc.* **2002**, *124*, 8530–8531.
(49) Mwaura, J.K.; Pinto, M.R.; Witker, D.; Ananthakrishnan, N.; Schanze, K.S.; Reynolds, J.R. *Langmuir* **2005**, *21*, 10119–10126.